Neurochemistry International 83-84 (2015) 28–40

Contents lists available at ScienceDirect

Neurochemistry International

journal homepage: www.elsevier.com/locate/nci

Magnetization transfer ratio does not correlate to myelin content in the brain in the MOG-EAE mouse model

Sveinung Fjær [a,b,*], Lars Bø [a,b], Kjell-Morten Myhr [a,b], Øivind Torkildsen [a,b], Stig Wergeland [a,b]

[a] KG Jebsen Centre for MS-Research, Department of Clinical Medicine, University of Bergen, Bergen, Norway
[b] The Norwegian Multiple Sclerosis Competence Centre, Department of Neurology, Haukeland University Hospital, Bergen, Norway

ARTICLE INFO

Article history:
Received 20 September 2014
Received in revised form 29 January 2015
Accepted 24 February 2015
Available online 2 March 2015

Keywords:
MTR
EAE
Myelin
Multiple sclerosis
Animal models

ABSTRACT

Magnetization transfer ratio (MTR) is a magnetic resonance imaging (MRI) method which may detect demyelination not detected by conventional MRI in the central nervous system of patients with multiple sclerosis (MS). A decrease in MTR value has previously been shown to correlate to myelin loss in the mouse cuprizone model for demyelination. In this study, we investigated the sensitivity of MTR for demyelination in the myelin oligodendrocyte (MOG) 1–125 induced experimental autoimmune encephalomyelitis (EAE) mouse model. A total of 24 female c57Bl/6 mice were randomized to a control group (N = 6) or EAE (N = 18). MTR images were obtained at a preclinical 7 Tesla Bruker MR-scanner before EAE induction (baseline), 17–19 days (midpoint) and 31–32 days (endpoint) after EAE induction. Mean MTR values were calculated in five regions of the brain and compared to weight, EAE severity score and myelin content assessed by immunostaining for proteolipid protein and luxol fast blue, lymphocyte and monocyte infiltration and iron deposition. Contrary to what was expected, MTR values in the EAE mice were higher than in the control mice at the midpoint and endpoint. No significant difference in myelin content was found according to histo- or immunohistochemistry. Changes in MTR values did not correlate to myelin content, iron content, lymphocyte or monocyte infiltration, weight or EAE severity scores. This suggest that MTR measures of brain tissue can give significant differences between control mice and EAE mice not caused by demyelination, inflammation or iron deposition, and may not be useful surrogate markers for demyelination in the MOG1-125 mouse model.

1. Introduction

Multiple sclerosis (MS) is a chronic disease of the central nervous system (CNS), characterized by inflammation, demyelination and axonal loss. Conventional magnetic resonance imaging (MRI) is crucial in the diagnostic workup of MS, showing hyperintense lesions on T2 weighted MRI. However, conventional MRI techniques are less sensitive to gray matter lesions and axonal loss, both representing pathophysiological mechanisms in MS which contribute significantly to disability progression of the disease. In the absence of reliable MRI markers of disability and progression in MS patients, magnetization transfer ratio (MTR) has been introduced as a semi-quantitative method that may be sensitive to change in myelin content in the CNS (Grossman, 1994). The MTR image is generated from the relative difference between two MR images (Dousset et al., 1992), differing only in the application of a pre-applied off-resonance saturation pulse that decreases signal intensity proportional to the density of macromolecules. Myelin is a lipid bilayer membrane abundant in the CNS, with a high macromolecule density susceptible to the offset MT-saturation pulse. MTR has been shown to decrease both in and in proximity of white matter MS lesions (Dousset et al., 1998; Filippi et al., 1995, 1998), and has detected gray matter changes in the MS brain, thus showing sensitivity to both demyelination and inflammation (Agosta et al., 2006; Vavasour et al., 2011). A 9.4 T post mortem study of formalin fixed MS brains showed a correlation between MTR and myelin content (Schmierer et al., 2010). MTR has been shown to correlate to both axonal density and myelin content from histopathological analyses of post-mortem tissue from brain- and spinal cord tissue of MS patients (Mottershead et al., 2003; Schmierer et al., 2004, 2007). In vivo detection of diffuse white matter abnormality is associated with decreased MTR, thought to be due to a decrease in myelin content (Laule et al., 2011). Studies in an experimental model of toxic demyelination with little or no perivascular inflammation, the cuprizone (CPZ) model, have found correlation between myelin content and MTR value (Boretius et al., 2012; Fjær et al., 2013;

* Corresponding author. KG Jebsen Centre for MS-Research, Department of Clinical Medicine, University of Bergen, Bergen, Norway. Tel.: +47 99445553; fax: +47 55975901.
E-mail address: sveinung@fjaer.com (S. Fjær).

http://dx.doi.org/10.1016/j.neuint.2015.02.006

Merkler et al., 2005; Zaaraoui et al., 2008). The CPZ model is, however, not a comprehensive model of MS pathophysiology, as it is characterized by demyelination in the absence of lymphocyte activation. Complementary to this is the experimental autoimmune encephalomyelitis (EAE), a model of CD8+ T lymphocyte mediated inflammation followed by demyelination, axonal degeneration and neuronal loss (Kuerten et al., 2007). The main CNS predilection site of EAE-induced inflammation is the spinal cord, and in the MOG-induced EAE there are some reports of lesions in the brain and cerebellum (Day, 2005). Accordingly, one study has shown a diffuse neurodegeneration of the brain and cerebellums of MOG-EAE mice (Mackenzie-Graham et al., 2011). In a study of MTR in brains of marmosets with EAE, MTR values decreased in lesions, but not in the cortex and normal appearing white matter (Blezer et al., 2007). In the EAE model in guinea pigs, a decrease in MTR values was shown both in the spinal cord and normal appearing white matter, but MTR did not correlate to myelin water in the brain (Gareau et al., 2000), and also showed correlation to axonal density and inflammation as well as to myelin in the spinal cord (Cook et al., 2004). MTR values has been shown to be lower in EAE induced rats compared to controls (Rausch et al., 2003), and rats in the acute phase has lower MTR values than those in a remitting phase (Berger et al., 2006). However, MTR values have been reported to decrease before demyelination, indicating that inflammatory processes also influence the MT effect (Serres et al., 2009, 2013). It has also been shown, by a quantitative magnetization transfer MRI model, that the changes in bound proton pool fraction (f*) was more pronounced than the changes in MTR in EAE induced rats (Rausch et al., 2009). A combined EAE-CPZ mouse model showed a stronger decrease in MTR than mouse only affected by CPZ, even though both groups showed similar amount of demyelination. The stronger decrease is thought to be due to axonal swelling, cellular infiltration and edema (Boretius et al., 2012). In mice with EAE induced by proteolipid protein, a decrease in MTR was seen in brainstem, cerebellum and frontal cortex, but not olfactory bulb (Mueggler et al., 2012). In a study of the effect of glatiramer acetate (GA) on EAE mice, the untreated EAE mice are shown to have lower MTR values than the GA treated (Aharoni et al., 2013). MTR is often considered to be mainly a marker of myelin change, but others argue that MTR is more closely related to neurodegenerative changes than to demyelination (Serres et al., 2009). In spite of previous efforts to study the pathophysiological correlations of changes in the MTR, questions remain with respect to the sensitivity of MTR in gray matter, and whether gray matter MTR is affected by diffuse neurodegeneration. The purpose of the present study was to examine whether MTR is a sensitive method for detecting demyelination in different brain regions in EAE mice, and to investigate how MTR values correlated to clinical disease activity.

2. Methods

2.1. Mice

A total of 24 female c57Bl/6 mice (Tacomic, Tornbjerg, Denmark) were acquired at 7 weeks of age with a mean weight of 22.7 ± *SD* 0.85*g*. During the acclimatization and experimental period, they were housed, 6 per cage, in Macrolon IVC-II cages (Scanbur, Karlslunde, Denmark) in standard laboratory conditions: light/dark cycles of 12/12*h*, cage temperature of 22.7 ± 1 °*C*, relative humidity of 52.9 ± 5% and 75 air changes per hour. They had ad libitum access to normal mouse chow ('Rat and mouse No. I' maintenance diet from Scanbur, Special Diet Services, Karlslunde, Denmark) and tap water during the acclimatization period of one week. Cage maintenance was performed once weekly by the same individuals throughout the study period. The experiment was conducted in accordance with the Federation of European Laboratory Animal Science Associations (FELASA) recommendations, and the protocol was approved by the Norwegian Animal Research Authority.

2.2. EAE induction

EAE was induced at post-immunization (p.i.) day 0 in 18 mice by s.c. injection of 25 *μg* of recombinant human myelin oligodendrocyte glycoprotein (MOG) (Hooke Labs, Lawrence, MA, USA) emulsified in Freund's complete adjuvant containing 1 mg/ml of Mycobacterium tuberculosis H37Ra (Sigma-Aldrich, St Louis, MO, USA). In addition, 200 *ng* of pertussis toxin (Sigma-Aldrich, St Louis, MO, USA) was administered intraperitoneally at p.i days 0 and 2.

2.3. Weight and clinical scoring

The mice were weighted twice weekly. Clinical scoring was assessed daily for signs of disease activity according to the following guidelines: grade 0, healthy; grade 1, tail weakness; grade 2, tail paralysis; grade 3, signs of hindlimb paresis; grade 4, evident hindlimb paresis; grade 5, marked hindlimb paralysis; grade 6, hindlimb paralysis; grade 7, tetraparalysis; grade 8, death due to EAE.

2.4. MRI protocol

The MRI experiments were performed on a 7 Tesla horizontal bore magnet (Pharmascan 70/16, Bruker BioSpin, Bruker Corporation, Germany) using a 23 mm ID mouse-head linear volume resonator. The mice were split into 4 groups. Three EAE exposed groups, EAE1, EAE2 and EAE3 (Ns = 6); and one control group, CTRL (N = 6). The mice were scanned at baseline (CTRL, EAE1, EAE2 and EAE3), before EAE induction; at the midpoint (CTRL, EAE2 and EAE3), 17–19 days after EAE induction; and at the endpoint (CTRL, EAE1 and EAE3), 31–32 days after EAE induction. Immediately after each mouse's last scan, they were sacrificed for histopathology (Table 1).

Table 1
Study setup.

	Baseline		EAE induction	Midpoint			Endpoint	
Day	–3	–2	0	17	18	19	31	32
CTRL	3	3		3	3		6*	
EAE1	3	3						6*
EAE2	3	3				6*		
EAE3	3	3		3	3			6*

Schematic representation of the study setup. The numbers show the number of animals from each group scanned at that day. The day is relative to EAE induction, baseline scans were done before induction, while the midpoint and endpoint scans were done after induction. *Marks that the animal was sacrificed for histology on the same day as being scanned.

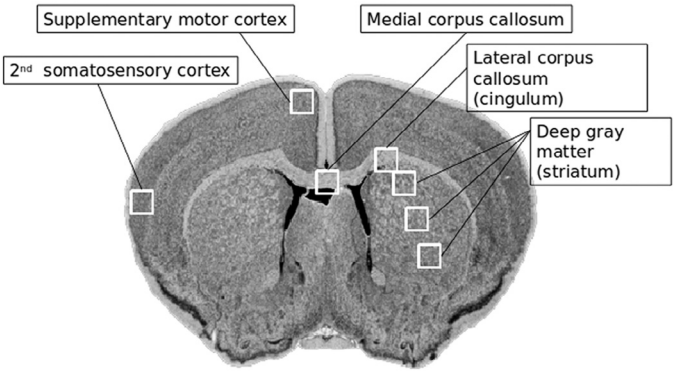

Fig. 1. Schematic illustration of brain tissue sections. Regions of the mouse brain analyzed by densitometry.

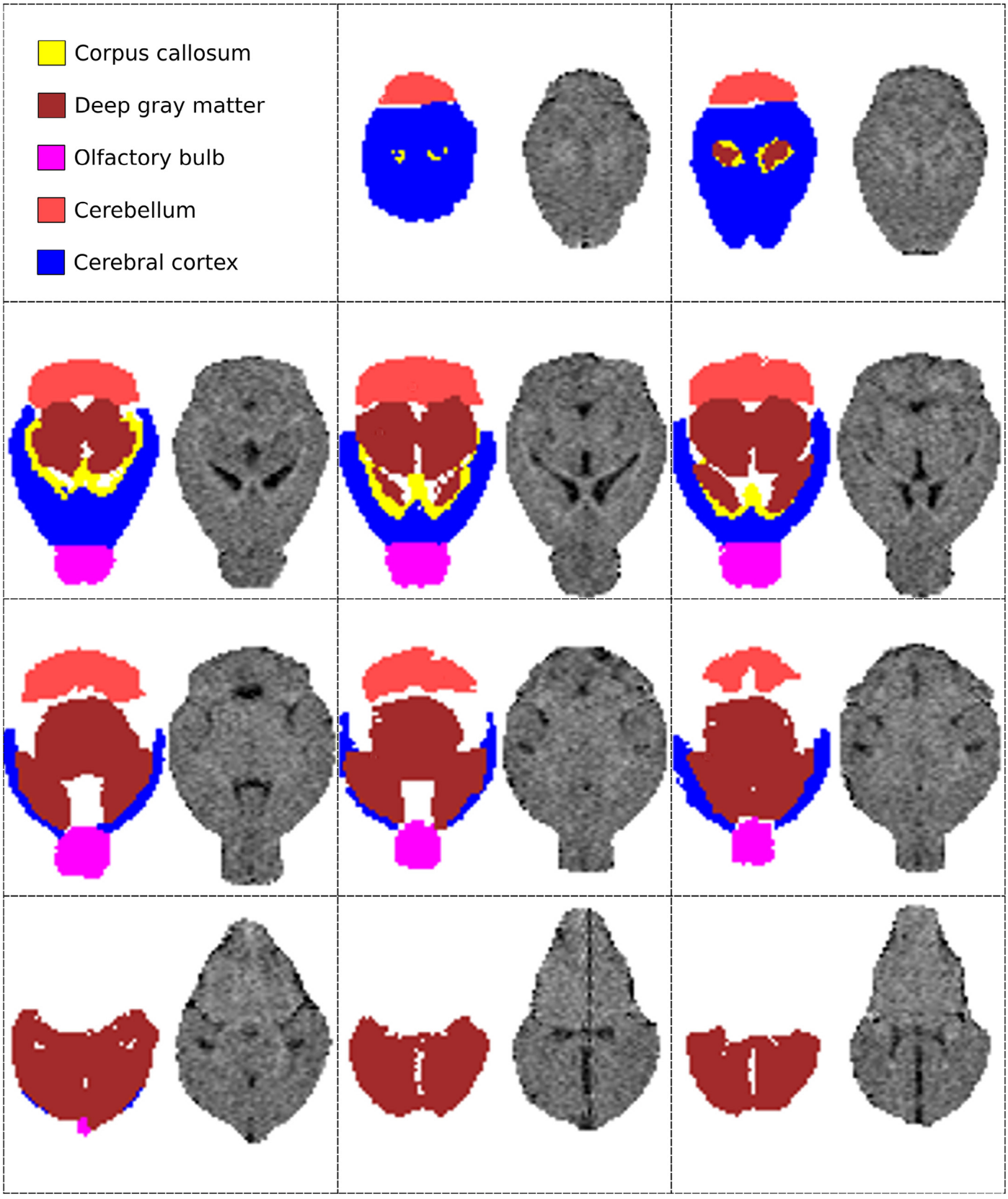

Fig. 2. MTR maps in which mean MTR values were calculated. Illustrated by an EAE mouse brain at EAE midpoint.

During scanning, the mice were anesthetized by 1.5% isoflurane in O_2, and the body temperature and respiratory frequency were monitored and kept constant at 37 ± 1.5 °C and 80 ± 20 respiratory cycles/min, respectively. The geometry was identical for all scans: $30 \times 128 \times 128$ matrix size, $2.56 \times 2.56 \times 0.7$ cm^3 FOV, giving $0.2 \times 0.2 \times 0.23$ mm^3 resolution. For the MTR acquisition, a FLASH sequence was used, with (M_s) and without (M_0) an offset magnetization transfer saturation pulse (–2000 *Hz* off resonance, Gaussian shaped, 10.4μT strength, 6.65*ms* duration, number of pulses: 1, 457 Hz bandwidth, 400 degree flip angle), 4 averages, TE = 2.3*ms*, TR = 28.5*ms* and flip angle = 10°. A T2-weighted (T2w) RARE image was acquired with 1 average, TE = 9*ms*, TR = 1500*ms* and a RARE factor of 16.

2.5. Preparation of brain tissue

Mice were euthanized by cardiac puncture in surgical anesthesia with fentanyl/fluanisone/midazolam; the brains were removed and fixated in 4% paraformaldehyde for at least 7 days, then paraffin embedded. Seven μm serial sections between areas 165 and 195 in the mouse brain atlas (http://www.hms.harvard.edu/research/brain) were analyzed. Sections were histochemically stained for myelin with Luxol fast blue (LFB). For immunohistochemistry, the sections were dewaxed and rehydrated before antigen retrieval in citrate buffer (pH 6.2). Sections were immunostained for myelin with anti-Proteolipid Protein antibody (PLP, Serotec, Oxford, UK),

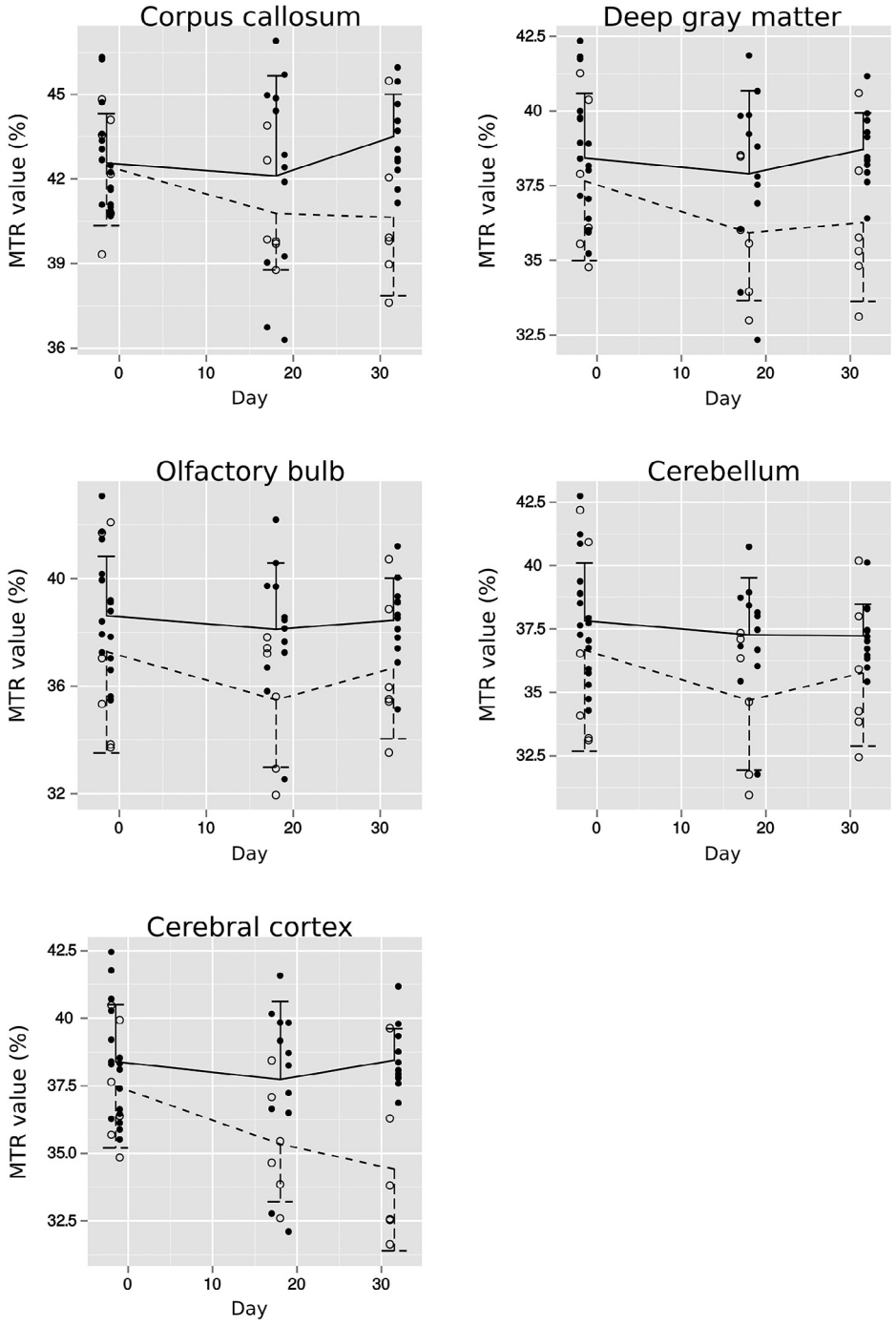

Fig. 3. Progression of MTR values over time. Mean MTR values in EAE induced mice (solid) and control animals (dashed). Dots (Filled: EAE mice. Open: Control mice) represent single MTR measurements. Error bars: standard deviation of mean MTR.

for activated macrophages and microglia with anti-Mac3 (BD Biosciences, Franklin Lakes, NJ, US) and for T-lymphocytes with anti CD3 (Sigma-Aldrich, St. Louis, MO, US). Sections were blocked with peroxidase blocking solution (Dako, Glostrup, Denmark), and visualized with EnVision 3.3 - diaminobenzidine (Dako, Glostrup, Denmark). The tissue sections were counterstained with hematoxylin. For each antibody, omission of the primary antibody served as negative control. Normal brain tissue from the healthy controls served as positive controls. Total (ferrous and non-ferrous) iron was detected using diaminobenzidine (DAB) enhanced Turnbulls staining, as described by Hametner et al. (2013).

2.6. Characterization of brain tissue

LFB sections were scored in a blinded manner by two observers, using light microscopy (Zeiss, Axio Imager A2, 40x, Oberkochen, Germany). For quantification of myelin loss, we used a semi-quantitative scoring system: no (0), minimal (0. 5), < 33% (1), 33–66% (2) and > 66% (3) demyelination. Immunopositivity and iron content were quantified by digital densiometry. Several sections of the corpus callosum, cerebral cortex and deep gray matter were photographed as indicated in Fig. 1, with identical exposure and brightness settings at 40× magnification (Zeiss AxioImager 2 with

Table 2
Region-wise comparison of MTR between groups.

Region	EAE vs Control			Acute vs chronic		
	EAE	Control	*p*-Value	Midpoint	Endpoint	*p*-Value
Corpus callosum	42.8 ± 2.8%	40.1 ± 2.3%	.03 (0.03)	42.1 ± 3.5%	43.5 ± 1.5%	.22 (1)
Deep gray matter	38.3 ± 2.1%	36.1 ± 2.4%	.007 (0.028)	37.9 ± 2.7%	38.7 ± 1.2%	.46 (1)
Olfactory bulb	38.3 ± 2.0%	36.1 ± 3.7%	.008 (0.028)	38.1 ± 2.5%	38.5 ± 1.6%	.69 (1)
Cerebellum	37.3 ± 1.7%	35.2 ± 2.7%	.01 (0.028)	37.3 ± 2.2%	37.2 ± 1.2%	.96 (1)
Cerebral cortex	38.1 ± 2.2%	34.9 ± 2.5%	.0004 (0.0015)	37.7 ± 2.9%	38.4 ± 1.1%	.44 (1)

ANOVA of MTR value, with first all EAE mice (from midpoint and endpoint) compared to their controls, then for the acute (midpoint) EAE group compared to the chronic (endpoint) EAE group. Mean values are presented with ± a standard deviation. *p*-Values from the ANOVA is presented, with Holm-corrected *p*-value in parenthesis.

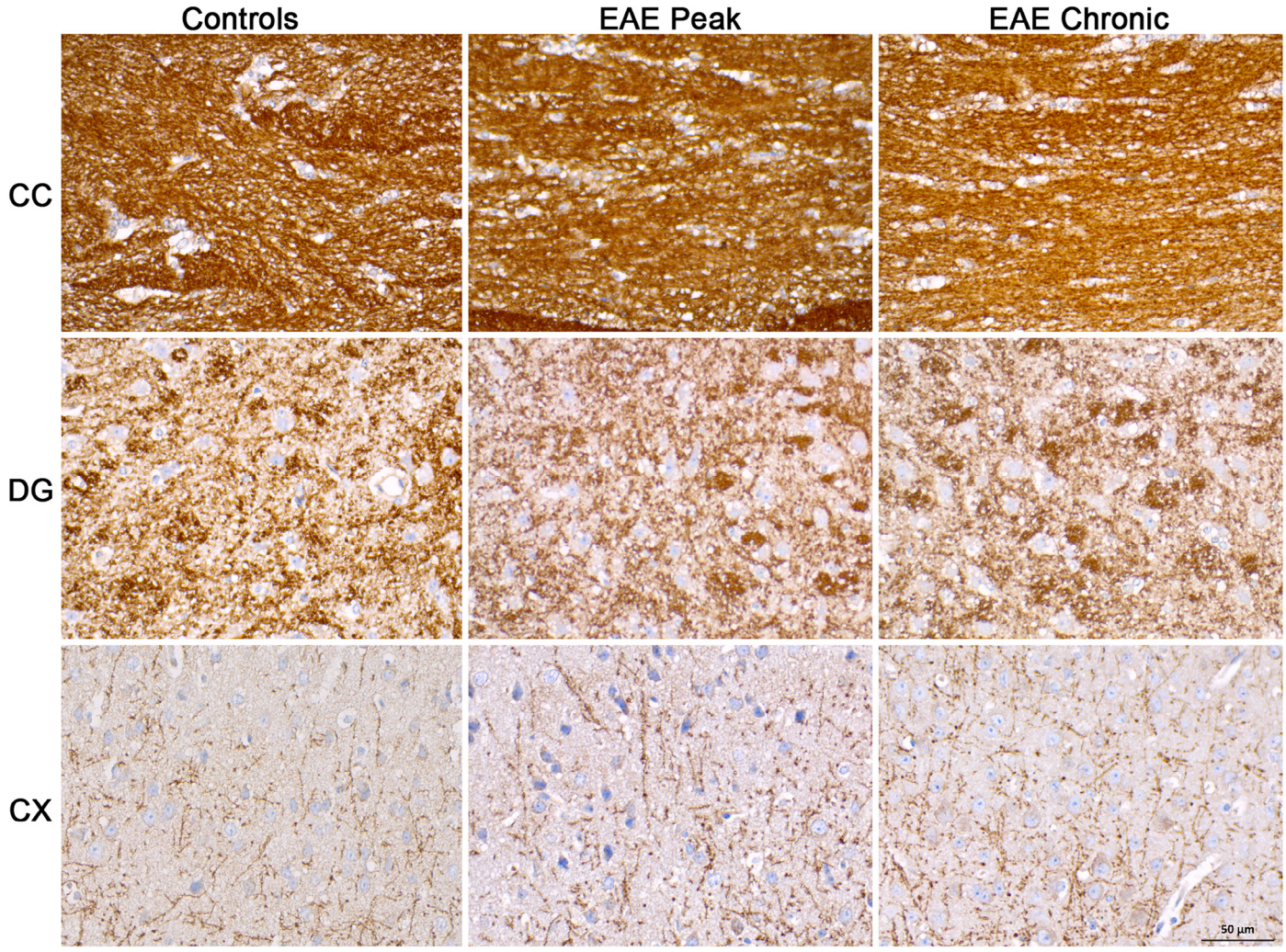

Fig. 4. Images of sections from corpus callosum (CC), deep gray matter (DG) and cerebral cortex (CX) immunostained for PLP, in controls, at peak EAE severity (EAE peak) and at EAE endpoint (EAE chronic). All images at 40×.

Zeiss AxioCam ERc 5s camera and Zeiss Zen 2012 ver 1.1.1 imaging software), and shadow-corrected. Using *Image processing and analysis in Java* (ImageJ ver. 1.48f, U. S. National Institutes of Health; Bethesda 2009), each grayscale image was manually thresholded by an experienced physician (SW) in order to avoid quantitative registration of low-intensity background staining. Hematoxylin staining was digitally removed by color deconvolution in ImageJ. The area of immunopositivity in each image was then calculated, and expressed as the percentage of pixels, or relative area, in each image with intensity within the threshold values. Finally, the region myelin content was calculated by averaging values for all images within the region.

2.7. MRI analysis

Images were analyzed using an in-house software written in Matlab (R2012a; The Mathworks, Natick, MA). Magnetization transfer ratio (MTR) was calculated using the formula: $MTR = 100 \times (M0 - Ms) / M0$. A semi-automatic method was used to segment the brains into anatomical regions. An anatomical segmentation map consisting of 5 brain regions (corpus callosum, deep gray matter, olfactory bulb, cerebellum and cerebral cortex) was drawn on the basis of the baseline T2w image (Fig. 2). This map was superimposed on all other subjects by linearly co-registering the T2w images using the Statistical Parametric Mapping 8 package (SPM8; Wellcome Trust Center for Neuroimaging, Oxford, England; http://www.fil.ion.ucl.ac.uk/spm). The mean MTR value was calculated in each region.

Table 3
Region-wise mean PLP area (myelin content).

Region	EAE vs control		
	EAE	Control	*p*-Value
Corpus callosum	80.4 ± 7.0%	83.3 ± 5.1%	.38(1)
Deep gray matter	48.7 ± 10.5%	48.3 ± 9.9%	.93(1)
Cerebral cortex	10.7 ± 3.4%	9.7 ± 1.4%	.53(1)

ANOVA of myelin content calculated as % of area stained with PLP in 4 locations in each of the three regions. Data presented only for the pooled data from the EAE mice compared to control mice. Mean values are presented with ± a standard deviation. *p*-Values from the ANOVA is presented, with Holm-corrected *p*-value in parenthesis.

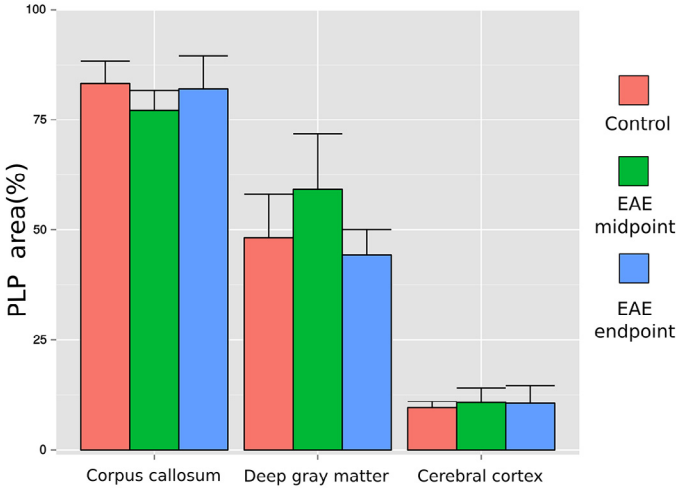

Fig. 5. % PLP area (myelin content). The mean myelin content from four different locations in corpus callosum, deep gray matter and cerebral cortex for the control mice, EAE mice at the midpoint and EAE mice at the endpoint. Error bars: standard deviation of PLP area.

2.8. Statistical analysis

Statistical analyses were done using R (RCore2012). Analysis of variance (ANOVA) was used to compare group differences. Comparison was done separately for the different brain regions, first comparing the EAE mice from midpoint and endpoint to the corresponding control mice (for MTR and weight, this was the control mice scanned/weighed at the same time point; for histological

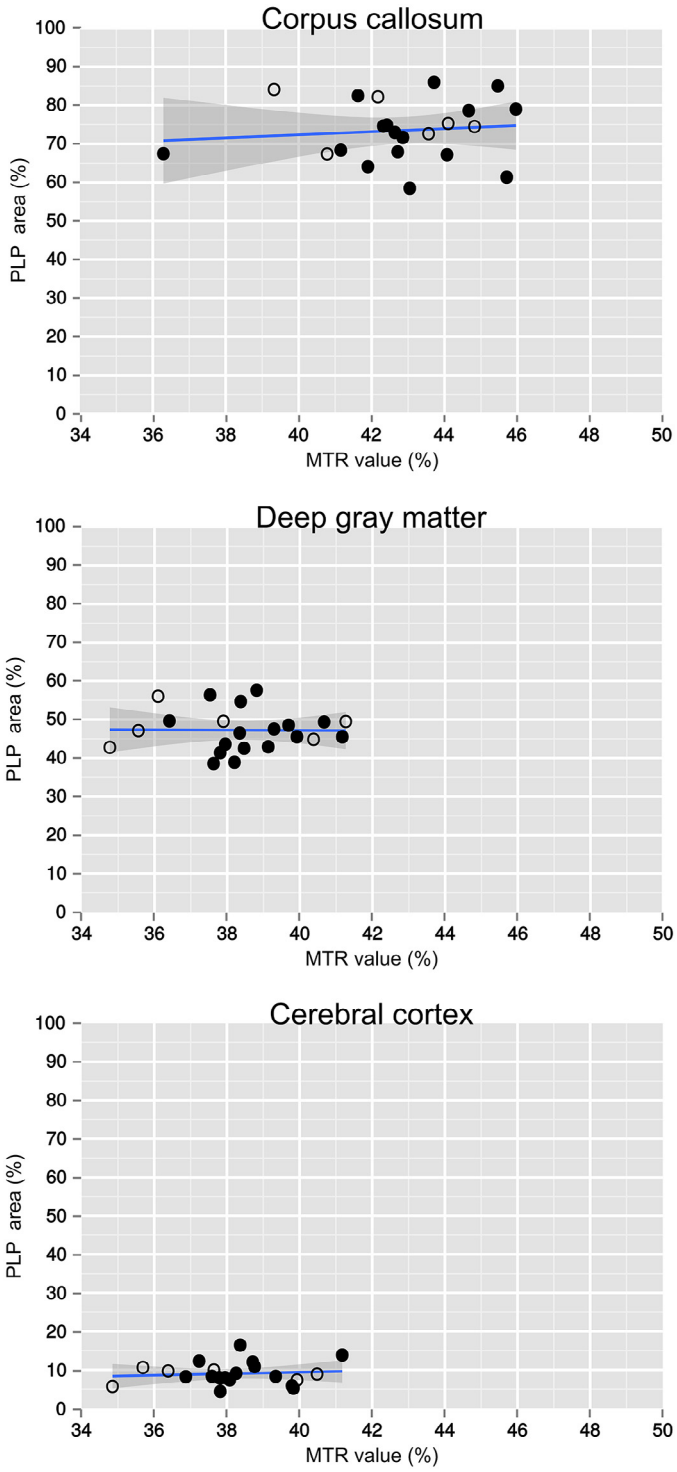

Fig. 6. Myelin content correlation to MTR values. Linear regression of myelin content, calculated from PLP stained brain tissue sections, and MTR values. Dots (Filled: EAE mice. Open: Control mice).

analysis, it was the tissue from the control mice from the endpoint); if a significant difference was seen, a secondary orthogonal comparison was done between the EAE mice from midpoint compared to EAE mice from endpoint. For the quantitative data (MTR, weight and PLP), the data were fitted with a linear model. For the LFB scoring, a generalized linear model was used. p-Values were Holm-adjusted to account for multiple comparisons. The MTR value was correlated to weight, EAE score and myelin content using linear regression. In addition, to compensate for variation in MTR value over time, a separate analysis was done using normalized MTR values. Normalization was done segment-wise and time point wise, by subtracting the mean MTR value of control animals. A $p < .05$ was considered significant.

3. Results

3.1. Region wise MTR values

Mean MTR values were significantly higher in EAE mice than in control mice in all regions after EAE induction, but no significant difference was seen between EAE mice at midpoint compared to the endpoint (Table 2 and Fig. 3). At baseline, EAE mice had non-significantly higher than control mice (corpus callosum: $\Delta MTR = 0.1\%$, $p = .90$; deep gray matter: $\Delta MTR = 0.7\%$, $p = .49$; olfactory bulb: $\Delta MTR = 1.3\%$, $p = .30$; cerebellum: $\Delta MTR = 1.2\%$, $p = .39$; cerebral cortex: $\Delta MTR = 0.9\%$, $p = .38$).

3.2. Myelin content

Myelin content assessed by immunohistochemical staining for PLP (Fig. 4) was not significantly different between the control mice and EAE mice in any of the regions (Table 3 and Fig. 5). PLP area did not correlate to MTR in any of the three areas assessed (corpus callosum: $R^2 = .01$, $p = .63$; deep gray matter: $R^2 = .08$, $p = .2$; cerebral cortex: $R^2 < .01$, $p = .97$) (Fig. 6)

Myelin content scored by immunohistochemical staining for LFB (Fig. 7) was not significantly different between the control mice and EAE mice in any of the regions (corpus callosum: $p = .29$; deep gray matter: $p = .29$; cerebral cortex: $p = .29$) (Fig. 8).

3.3. Lymphocyte infiltration and iron accumulation

No infiltration of CD3 immunopositive lymphocytes was observed in the examined brain tissue regions. Iron deposition could not be detected in brain tissue from neither EAE nor control mice (Fig. 9). Thus, no differences in iron content were detected between the EAE mice and control mice in deep gray matter, corpus callosum or cerebral cortex.

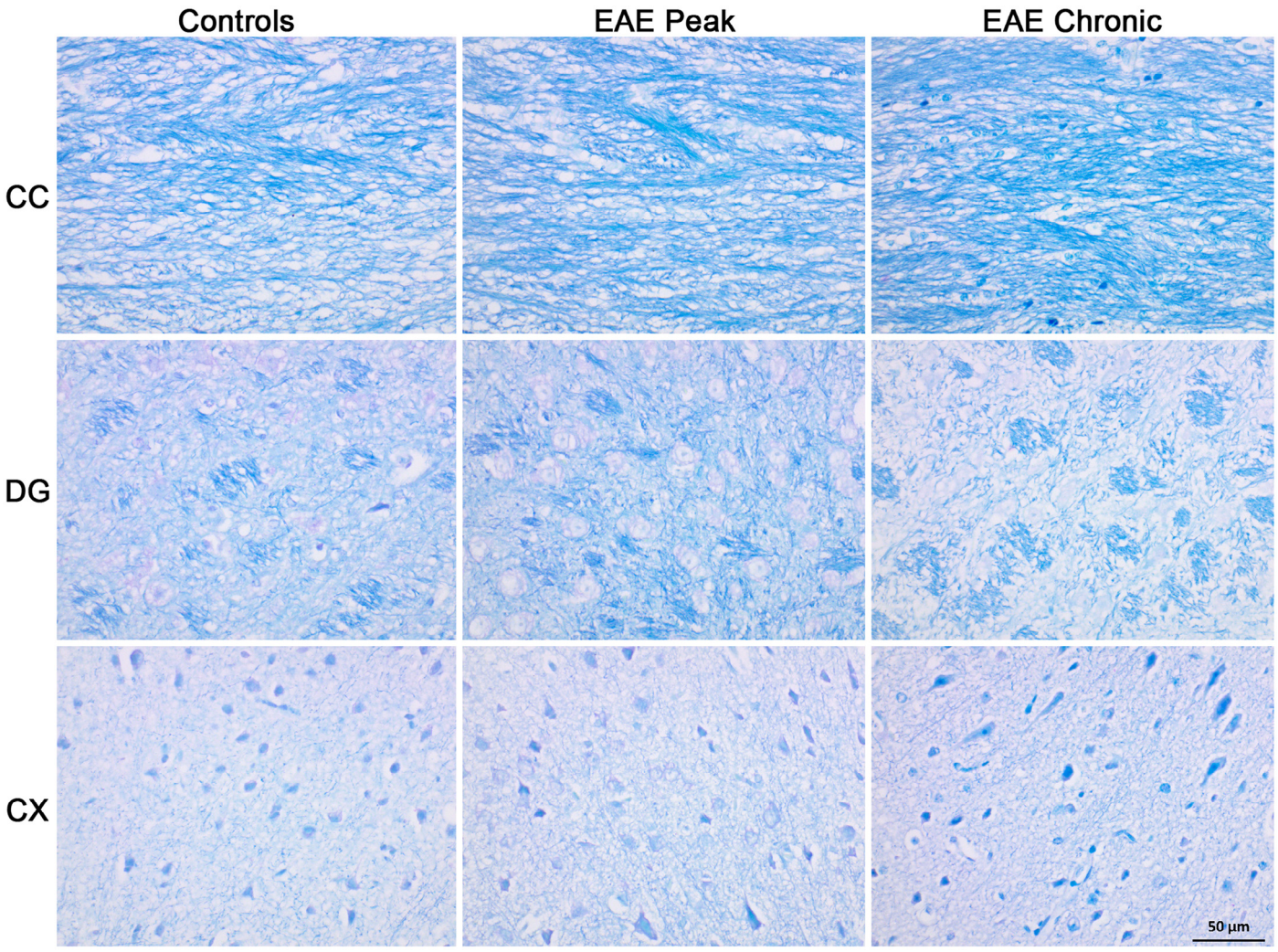

Fig. 7. Images of sections from corpus callosum (CC), deep gray matter (DG) and cerebral cortex (CX) immunostained for LFB, in controls, at peak EAE severity (EAE peak) and at EAE endpoint (EAE chronic). All images at 40×.

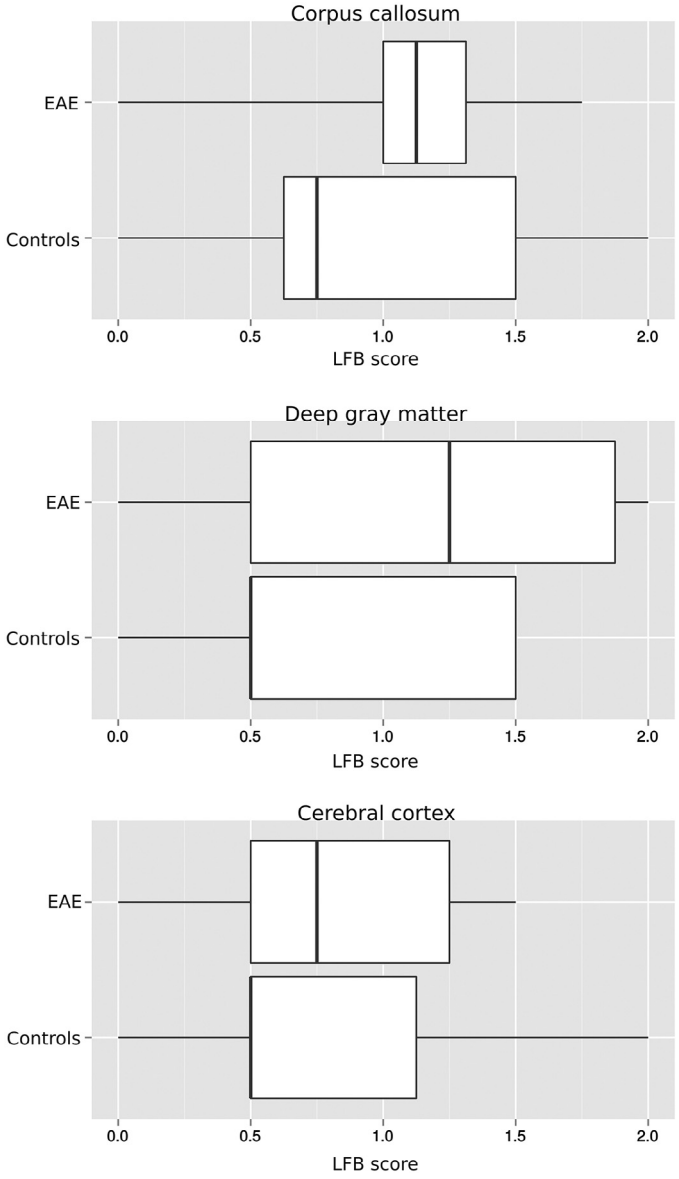

Fig. 8. LFB score (myelin content). Box plot of distribution of LFB scores in corpus callosum, deep gray matter and cerebral cortex for control mice and EAE mice. The box plot represents minimum value, lower quartile, median, upper quartile and maximum value.

3.4. Weight and clinical scoring

Control mice was significantly heavier than EAE mice, while the chronic EAE mice at endpoint was heavier than the acute EAE mice at midpoint (Table 4 and Fig. 10A). No correlation between MTR values and weight was found ($R^2 < .01$ for all regions) (Fig. 11). The clinical score showed that EAE induced mice had increasing disease severity from p.i. day 10 to 17, followed by an incomplete remission (Fig. 10B). No correlations between MTR values and cumulative clinical scores were found (corpus callosum: $R^2 = .03$, $p = .42$; deep gray matter: $R^2 = .02$, $p = .53$; olfactory bulb: $R^2 = .01$, $p = .60$; cerebellum: $R^2 < .01$, $p = .99$; cerebral cortex: $R^2 = .01$, $p = .63$) (Fig. 12). Analyses of non-cumulative clinical scores and normalized cumulative clinical scores did not change the results.

All analyses were, in addition, done using normalized MTR values, giving similar results (data not shown).

Table 4
Mean weight over time.

EAE vs control			Acute vs chronic		
EAE	Control	*p*-Value	Midpoint	Endpoint	*p*-Value
21.3 ± 2.3g	23.0 ± 1.3g	.02	20.2 ± 2.0g	22.8 ± 1.6g	.001

ANOVA of weight, with first all EAE mice (from midpoint and endpoint) compared to their controls, then for the acute (midpoint) EAE group compared to the chronic (endpoint) EAE group. Mean values are presented with ± a standard deviation.

4. Discussion

We have shown an unexpected increase in MTR value in the brains of mice with MOG-EAE as compared to controls that do not correlate to histopathological changes. MTR is considered to be a semi-quantitative measure of myelin content, and a decrease in MTR has previously been reported in a few other EAE studies (Aharoni et al., 2013; Gareau et al., 2000; Rausch et al., 2003; Serres et al., 2009). These studies, however, did not correlate MTR values to quantitative immunohistochemical measures.

In line with a previous study (Mackenzie-Graham et al., 2011), we expected diffuse neurodegeneration and demyelination in the brain of the EAE mice, and was interested in whether this could be detected by a corresponding decrease in MTR values. There was, however, no evidence for diffuse demyelination in our study, and contrary to our expectations, the MTR value increased in EAE mice. A difference in myelin content can probably not explain the increase in MTR value in EAE mice compared to the controls. This suggests that other methodological or pathophysiological mechanisms affect the MTR values.

The segmentation of the MR images was done using linear co-registration. Dehydration could change the morphology in the EAE mouse brains, requiring a non-linear approach. We did not notice any such problems in this study, and small misregistration would not significantly change the results since large 3D segments were used. In our data, we observed a variation in the MTR values in the control mice over time, which we would not expect from a physiological point of view. In a previous study (Fjær et al., 2013), we experienced a non-biological variation of the MTR value of control animals over the span of eight weeks in the range 2%–5%. From this experience, we expected to see some variation over a span of four weeks, but we have stable MTR values over a span of 2–3 days. A weakness in our study design is that we had to scan the mice over several days. In particular, we scanned all the control mice the same day. It is possible that the group differences seen in this study is due to an error in the MTR value which is actually dependent on the day the mice were scanned. To the best of our knowledge, the relevant external factors were controlled for the following: M0 and MT were always acquired with the same settings on the scanner, without recalibrations between the two acquisitions; the receiver gain was kept constant in all MTR acquisitions at all times; the temperature of the animals, and the room, was held relatively constant; images were reconstructed from raw data to control for changes that could occur in on-scanner conversion.

MTR has been reported as a sensitive and specific indicator for myelin content. As no significant difference in myelin content was found between EAE mice and control mice, we might not expect a clear correlation between MTR and myelin content, as we have previously demonstrated in the cuprizone model (Fjær et al., 2013). The lack of a significant demyelination may also explain why we did not see the same correlations as in previous studies of EAE model in marmosets (Blezer et al., 2007) and guinea pigs (Cook et al., 2004; Gareau et al., 2000).

Iron has been shown to affect the magnetization transfer effect in the brain (Smith et al., 2009), and has been exploited in MTR

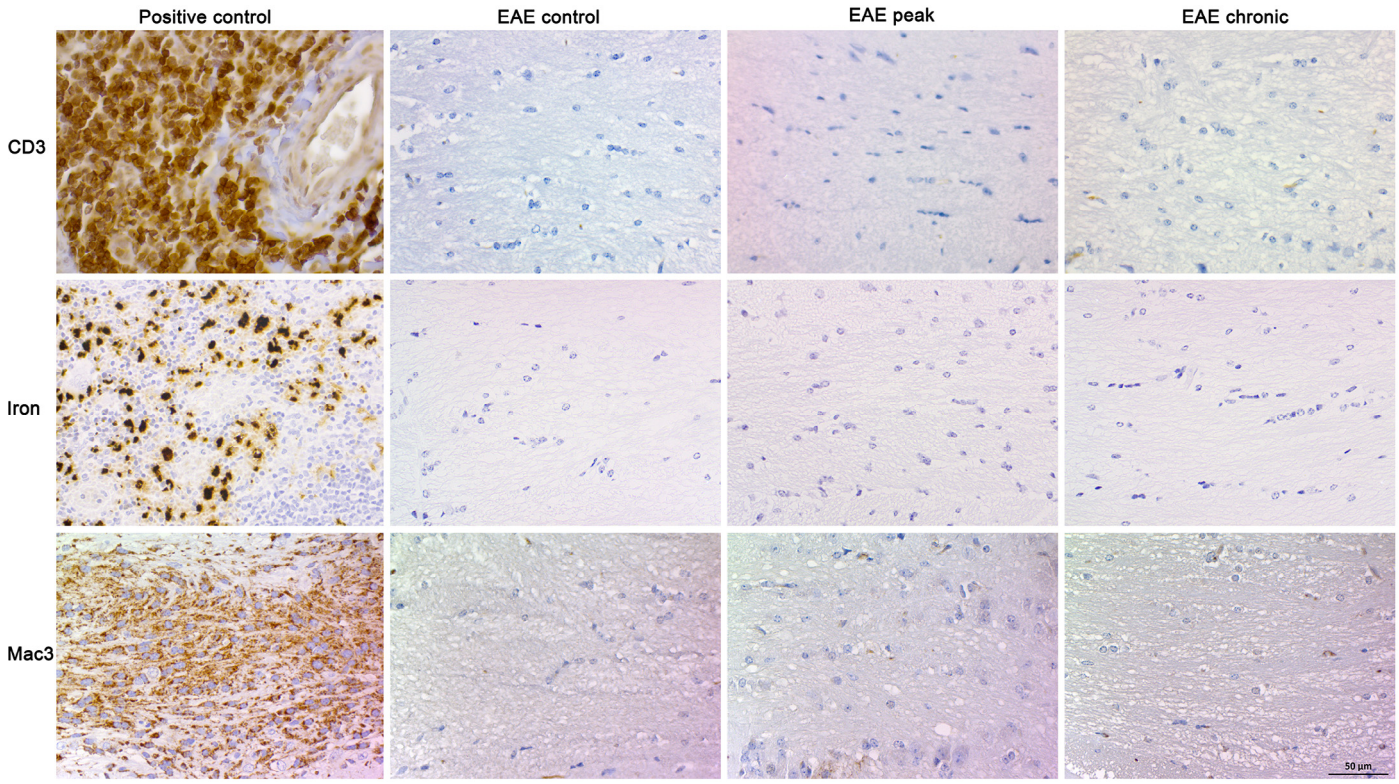

Fig. 9. Representative images of sections from positive controls, and from corpus callosum in control mice (EAE control), at peak EAE severity (EAE peak), and at EAE endpoint (EAE chronic). Upper row: Immunostained for CD3 positive T-lymphocytes. Positive control: Tonsil. Mid row: Turnbulls DAB-enhanced iron stain. Positive control: Spleen. Lower row: Immunostained for activated microglia and macrophages (Mac3). Positive control: cuprizone-exposed mouse brain. There were no signs of lymphocyte infiltration, iron deposition or microglia activation in any of the investigated regions at neither time point. All images at 40×.

imaging of rectal cancer to detect fibrosis (Martens et al., 2014; Papanikolaou et al., 2000). It has been suggested that iron is an important indicator of different physiological and pathological processes in MS (Bagnato et al., 2013), and we therefore investigated whether iron could have influenced out MTR changes. We could, however, not detect any differences in iron content between EAE induced mice and control mice by Turnbull's DAB-enhanced iron staining, making it unlikely that iron influenced our MTR findings. This is supported by a recent study reporting no evidence of iron accumulation, other than in single iron-containing perivascular or meningeal macrophages in individual lesions in MOG induced EAE mice (Schuh et al., 2014). In our study, we did not find any Mac-3 immunopositive activated microglia or macrophages in the brain tissue sections. In MOG1-125 induced EAE, the degree of inflammation and demyelination in the brain is variable compared to the more typical affection of the spinal cord. If present in the brain, lesions occur more frequently in the caudal aspects and in the cerebellum than in the frontal parts. As such, we do not find that the absence of lymphocyte infiltration and microglial activation is atypical in our experiment. Dehydration is another factor that can influence MTR values, as the pools of water affected by magnetization transfer may change relatively in size. This effect was recently exploited in a study employing magnetization transfer to show changes in hydration state in the achilles tendons (Syha et al., 2014). MTR has shown a stronger, inverse correlation with total water content ($r = -.65$) than to myelin water content ($r = -.36$) (Vavasour et al., 2011). In EAE models, dehydration has been shown primarily in the spinal cord, but smaller degrees of dehydration has also been seen in the brain, with sicker animals having higher degree of dehydration (Orr et al., 1994). We used weight measures as a surrogate indicator of dehydration, but did not detect any correlation between weight and MTR values, indicating that a hydration effect probably did not influence MTR

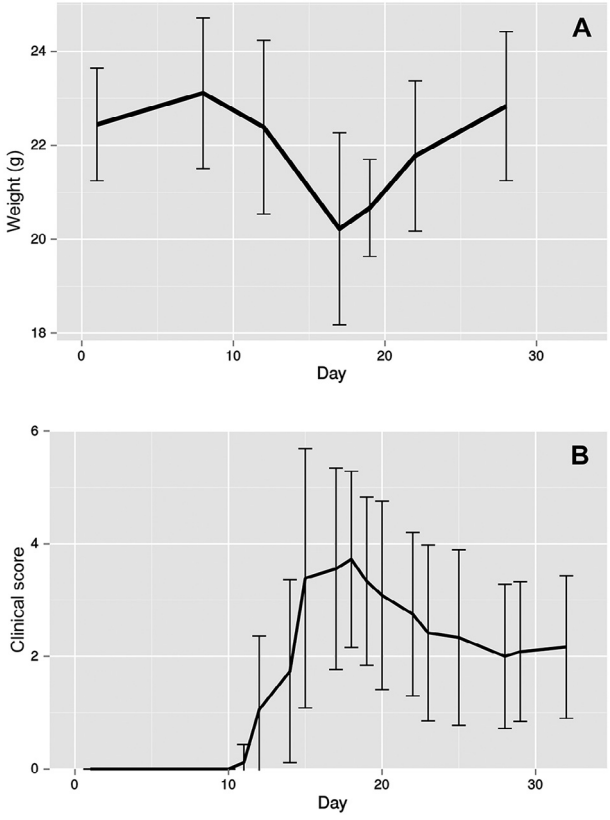

Fig. 10. Weight and disease score over time in EAE induced mice. Line represents group mean weight/clinical score. Error bars: Standard deviation of weight/clinical score. A: Body weight in grams. B: Clinical disease score.

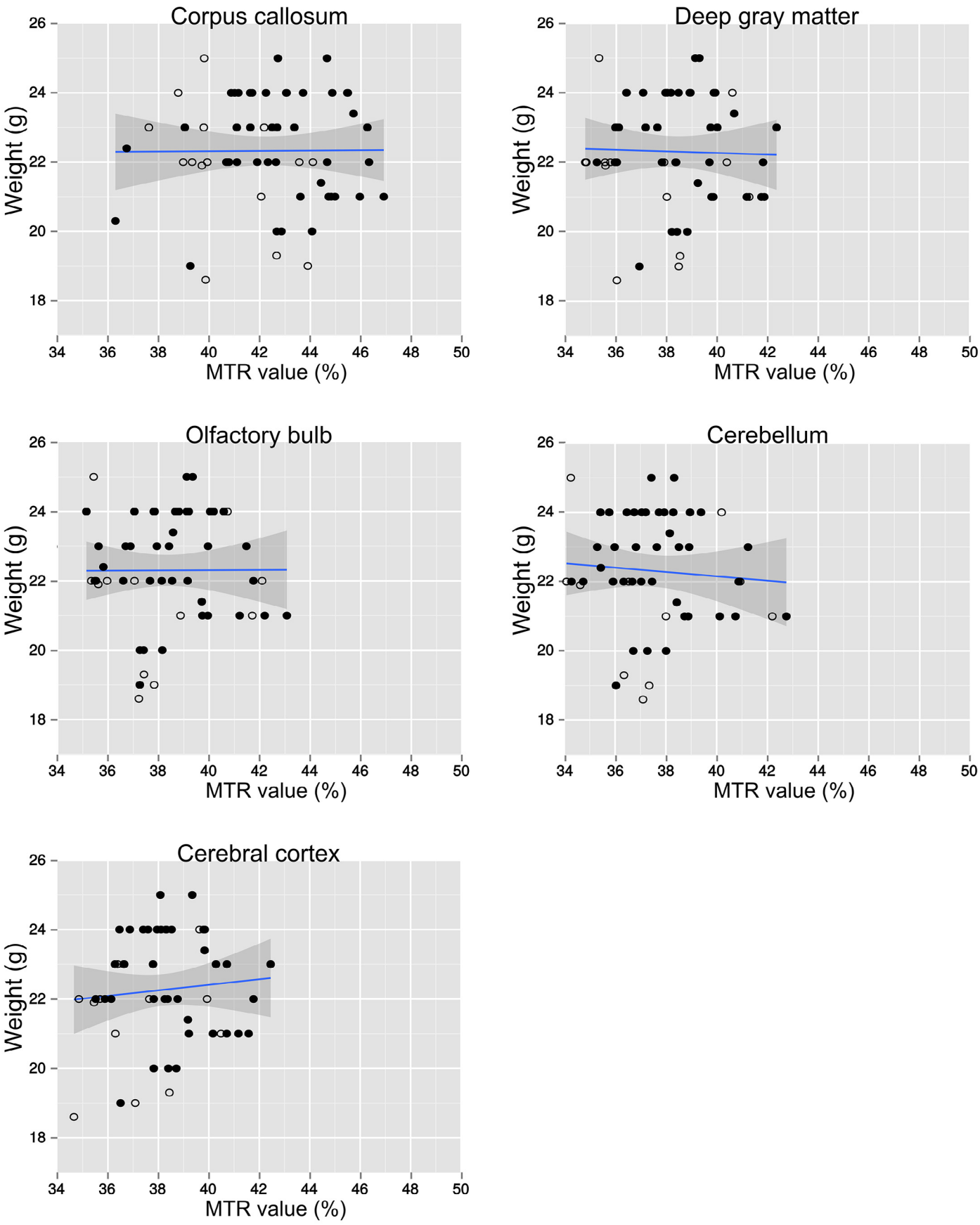

Fig. 11. Correlation between weight and MTR value. Dots (Filled: EAE mice. Open: Control mice).

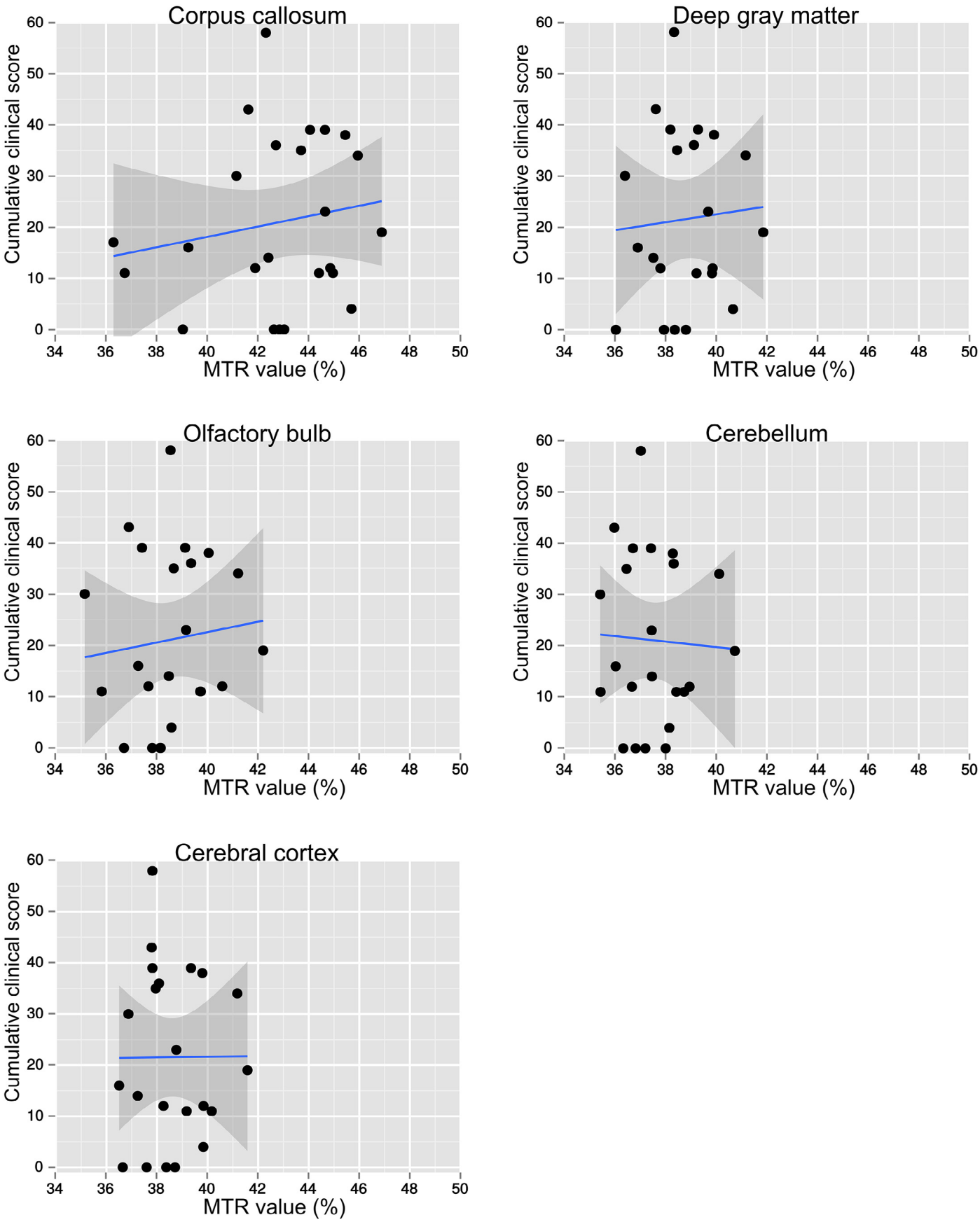

Fig. 12. Correlation between cumulative clinical scores and MTR values. Dots represent EAE mice scanned at the midpoint and the endpoint.

changes observed in our study. A study of hypo- and isointense T1 lesions in MS brains suggests that a lower MTR in hypointense lesions is not due to lower myelin content, but to axonal loss (Vavasour et al., 2007), which is supported by a study on MS lesions showing a higher correlation between MTR and axonal density than to myelin content (van Waesberghe et al., 1999). Axonal density was not examined in our study, but was not expected to be higher in the EAE induced mice compared to control mice. It was therefore unlikely that axonal density influenced our MTR findings.

If MTR change would be sensitive to diffusely damaged brain matter, we would expect to see a correlation between the severity of disease in the EAE mice and MTR values. No such correlation was observed in our study, implying that MTR of the brain done in this study had no predictive value for the severity of the disease. To our knowledge, a correlation between MTR and clinical disease score in the EAE mouse model has not been reported in other studies either. The spinal cord is important in the pathology of the EAE mice. We did not do spinal cord MTR, and can thus not say anything about the sensitivity of spinal cord MTR on myelin content. Acquisition parameters for MTR on preclinical MRI scanners have not been standardized. Both spin-echo and flash sequences are being used, with a range of repetition times, echo times and flip angles. A Gaussian shaped off-resonance pulse is most common, but the offset frequency varies from 1000 Hz (Rausch et al., 2009) to 5000 Hz (Boretius et al., 2012), and it is typically not noted explicitly whether the offset is positive, negative or both. The strength, saturation time, flip angle, bandwidth and number of saturation pulses are also variable, and often not reported in research papers. The acquisition parameters used in this study is similar to that of other MTR studies done on 7 Tesla preclinical scanners (Boss et al., 2008; Fjær et al., 2013; Rausch et al., 2009), with the possible exception that this study used a negative offset frequency (this is not explicitly denoted in the other studies). The negative offset should theoretically make a qualitatively difference, as it is the broader eigenfrequency spectrum of the macromolecules that causes the MT effect, rather than a chemical shift. Thus, we did not expect that the acquisition parameters used in this study would be the cause of the observed increase in MTR values in EAE mice.

EAE can be induced in several different ways, giving different disease progress and pathology (Kuerten et al., 2007). To our knowledge, only one previous MTR study on MOG induced EAE in mice has been reported (Aharoni et al., 2013). This study did not show the same disease progress in the EAE mice as observed in our study. Whereas they reached a plateau in disease severity 17 days after EAE induction, we saw a remission of the disease 17 days after EAE induction, also followed by an increase in weight and myelin content. They found that the EAE induced mice had significant lower mean MTR value than a control group in several regions from 13 days to 27 days after induction, but no correlation tests between MTR values and myelin content from immunohistopathology examinations were reported. Their MTR measurements were done using a 9.4 Tesla preclinical MRI scanner, using a spin-echo sequence.

In our study, we have seen that MTR values increase in MOG1-125 EAE mice compared to control mice, and that MTR does not correlate to myelin content or disease severity score. We have explored possible causes for our findings, showing that weight/dehydration and iron deposits probably did not affect the results. A possible variation in MTR value from day to day may have caused false significant results. The EAE induced mice showed a typical disease course, shown in previous studies, and the MTR acquisition parameters was similar to those used in other preclinical MTR studies, but we did not see significant changes in myelin content in histopathology. Our findings indicate that MTR measures of the brain can give significant differences between control mice and EAE mice not caused by known pathology, and may not be useful surrogate markers for demyelination in the MOG1-125 mouse model.

References

Agosta, F., Rovaris, M., Pagani, E., Sormani, M.P., Comi, G., Filippi, M., 2006. Magnetization transfer MRI metrics predict the accumulation of disability 8 years later in patients with multiple sclerosis. Brain 129 (Pt 10), 2620–2627. doi:10.1093/brain/awl208; <http://dx.doi.org/10.1093/brain/awl208>.

Aharoni, R., Sasson, E., Blumenfeld-Katzir, T., Eilam, R., Sela, M., Assaf, Y., et al., 2013. Magnetic resonance imaging characterization of different experimental autoimmune encephalomyelitis models and the therapeutic effect of glatiramer acetate. Exp. Neurol. 240, 130–144. doi:10.1016/j.expneurol.2012.11.004; <http://dx.doi.org/10.1016/j.expneurol.2012.11.004>.

Bagnato, F., Hametner, S., Welch, E.B., 2013. Visualizing iron in multiple sclerosis. Magn. Reson. Imaging 31 (3), 376–384. doi:10.1016/j.mri.2012.11.011; <http://dx.doi.org/10.1016/j.mri.2012.11.011>.

Berger, C., Hiestand, P., Kindler-Baumann, D., Rudin, M., Rausch, M., 2006. Analysis of lesion development during acute inflammation and remission in a rat model of experimental autoimmune encephalomyelitis by visualization of macrophage infiltration, demyelination and blood-brain barrier damage. NMR Biomed. 19 (1), 101–107. doi:10.1002/nbm.1007; <http://dx.doi.org/10.1002/nbm.1007>.

Blezer, E.L.A., Bauer, J., Brok, H.P.M., Nicolay, K., 't't Hart, B.A., 2007. Quantitative MRI-pathology correlations of brain white matter lesions developing in a non-human primate model of multiple sclerosis. NMR Biomed. 20 (2), 90–103. doi:10.1002/nbm.1085; <http://dx.doi.org/10.1002/nbm.1085>.

Boretius, S., Escher, A., Dallenga, T., Wrzos, C., Tammer, R., Brück, W., et al., 2012. Assessment of lesion pathology in a new animal model of ms by multiparametric MRI and DTI. Neuroimage 59 (3), 2678–2688. doi:10.1016/j.neuroimage.2011.08.051; <http://www.sciencedirect.com/science/article/pii/S1053811911009682>.

Boss, A., Oppitz, M., Wehrl, H.F., Rossi, C., Feuerstein, M., Claussen, C.D., et al., 2008. Measurement of t1, t2, and magnetization transfer properties during embryonic development at 7 Tesla using the chicken model. J. Magn. Reson. Imaging 28 (6), 1510–1514. doi:10.1002/jmri.21601; <http://dx.doi.org/10.1002/jmri.21601>.

Cook, L.L., Foster, P.J., Mitchell, J.R., Karlik, S.J., 2004. In vivo 4.0-t magnetic resonance investigation of spinal cord inflammation, demyelination, and axonal damage in chronic-progressive experimental allergic encephalomyelitis. J. Magn. Reson. Imaging 20 (4), 563–571. doi:10.1002/jmri.20171; <http://dx.doi.org/10.1002/jmri.20171>.

Day, M., 2005. Histopathology of eae. In: Lavi, E., Constantinescu, C. (Eds.), Experimental Models of Multiple Sclerosis, Springer US. pp. 25–43. doi:10.1007/0-387-25518-4 <http://dx.doi.org/10.1007/0-387-25518-4>.

Dousset, V., Grossman, R.I., Ramer, K.N., Schnall, M.D., Young, L.H., Gonzalez-Scarano, F., et al., 1992. Experimental allergic encephalomyelitis and multiple sclerosis: lesion characterization with magnetization transfer imaging. Radiology 182 (2), 483–491. <http://dx.doi.org/10.1148/radiology.182.2.1732968>.

Dousset, V., Gayou, A., Brochet, B., Caille, J.M., 1998. Early structural changes in acute ms lesions assessed by serial magnetization transfer studies. Neurology 51 (4), 1150–1155. doi:10.1212/WNL.51.4.1150.

Filippi, M., Campi, A., Dousset, V., Baratti, C., Martinelli, V., Canal, N., et al., 1995. A magnetization transfer imaging study of normal-appearing white matter in multiple sclerosis. Neurology 45 (3 Pt 1), 478–482. doi:10.1212/WNL.45.3.478.

Filippi, M., Rocca, M.A., Comi, G., 1998. Magnetization transfer ratios of multiple sclerosis lesions with variable durations of enhancement. J. Neurol. Sci. 159 (2), 162–165. doi:10.1016/S0022-510X(98)00162-2.

Fjær, S., Bø, L., Lundervold, A., Myhr, K.-M., Pavlin, T., Torkildsen, O., et al., 2013. Deep gray matter demyelination detected by magnetization transfer ratio in the cuprizone model. PLoS ONE 8 (12), e84162. doi:10.1371/journal.pone.0084162; <http://dx.doi.org/10.1371/journal.pone.0084162>.

Gareau, P.J., Rutt, B.K., Karlik, S.J., Mitchell, J.R., 2000. Magnetization transfer and multicomponent t2 relaxation measurements with histopathologic correlation in an experimental model of ms. J. Magn. Reson. Imaging 11 (6), 586–595. doi:10.1002/1522-2586(200006)11:6<586::aid-jmri3>3.0.CO;2-V.

Grossman, R.I., 1994. Magnetization transfer in multiple sclerosis. Ann. Neurol. 36 (Suppl.), S97–S99. doi:10.1002/ana.410360722.

Hametner, S., Wimmer, I., Haider, L., Pfeifenbring, S., Brück, W., Lassmann, H., 2013. Iron and neurodegeneration in the multiple sclerosis brain. Ann. Neurol. 74 (6), 848–861. doi:10.1002/ana.23974; <http://dx.doi.org/10.1002/ana.23974>.

Kuerten, S., Kostova-Bales, D.A., Frenzel, L.P., Tigno, J.T., Tary-Lehmann, M., Angelov, D.N., et al., 2007. Mp4- and mog:35–55-induced eae in c57bl/6 mice differentially targets brain, spinal cord and cerebellum. J. Neuroimmunol. 189 (1–2), 31–40. doi:10.1016/j.jneuroim.2007.06.016; <http://dx.doi.org/10.1016/j.jneuroim.2007.06.016>.

Laule, C., Vavasour, I.M., Leung, E., Li, D.K.B., Kozlowski, P., Traboulsee, A.L., et al., 2011. Pathological basis of diffusely abnormal white matter: insights from magnetic resonance imaging and histology. Mult. Scler. 17 (2), 144–150. doi:10.1177/1352458510384008; <http://dx.doi.org/10.1177/1352458510384008>.

Mackenzie-Graham, A., Rinek, G.A., Avedisian, A., Gold, S.M., Frew, A.J., Aguilar, C., et al., 2011. Cortical atrophy in experimental autoimmune encephalomyelitis: in vivo imaging. Neuroimage 60 (1), 95–104. doi:10.1016/j.neuroimage.2011.11.099; <http://dx.doi.org/10.1016/j.neuroimage.2011.11.099>.

Martens, M.H., Lambregts, D.M.J., Papanikolaou, N., Heijnen, L.A., Riedl, R.G., zur Hausen, A., et al., 2014. Magnetization transfer ratio: a potential biomarker for the assessment of postradiation fibrosis in patients with rectal cancer. Invest. Radiol. 49 (1), 29–34. doi:10.1097/RLI.0b013e3182a3459b; <http://dx.doi.org/10.1097/RLI.0b013e3182a3459b>.

Merkler, D., Boretius, S., Stadelmann, C., Ernsting, T., Michaelis, T., Frahm, J., et al., 2005. Multicontrast MRI of remyelination in the central nervous system. NMR Biomed. 18 (6), 395–403. doi:10.1002/nbm.972; <http://dx.doi.org/10.1002/nbm.972>.

Mottershead, J.P., Schmierer, K., Clemence, M., Thornton, J.S., Scaravilli, F., Barker, G.J., et al., 2003. High field MRI correlates of myelin content and axonal density in multiple sclerosis–a post-mortem study of the spinal cord. J. Neurol. 250 (11), 1293–1301. doi:10.1007/s00415-003-0192-3; <http://dx.doi.org/10.1007/s00415-003-0192-3>.

Mueggler, T., Pohl, H., Baltes, C., Riethmacher, D., Suter, U., Rudin, M., 2012. MRI signature in a novel mouse model of genetically induced adult oligodendrocyte cell death. Neuroimage 59 (2), 1028–1036. doi:10.1016/j.neuroimage.2011.09.001; <http://dx.doi.org/10.1016/j.neuroimage.2011.09.001>.

Orr, E.L., Aschenbrenner, J.E., Oakford, L.X., Jackson, F.L., Stanley, N.C., 1994. Changes in brain and spinal cord water content during recurrent experimental autoimmune encephalomyelitis in female lewis rats. Mol. Chem. Neuropathol. 22 (3), 185–195. doi:10.1007/BF03160105.

Papanikolaou, N., Ghiatas, A., Kattamis, A., Ladis, C., Kritikos, N., Kattamis, C., 2000. Non-invasive myocardial iron assessment in thalassaemic patients. t2 relaxometry and magnetization transfer ratio measurements. Acta Radiol. 41 (4), 348–351. doi:10.1080/028418500127345442.

Rausch, M., Hiestand, P., Baumann, D., Cannet, C., Rudin, M., 2003. MRI-based monitoring of inflammation and tissue damage in acute and chronic relapsing eae. Magn. Reson. Med. 50 (2), 309–314. doi:10.1002/mrm.10541; <http://dx.doi.org/10.1002/mrm.10541>.

Rausch, M., Tofts, P., Lervik, P., Walmsley, A., Mir, A., Schubart, A., et al., 2009. Characterization of white matter damage in animal models of multiple sclerosis by magnetization transfer ratio and quantitative mapping of the apparent bound proton fraction f. Mult. Scler. 15 (1), 16–27. doi:10.1177/1352458508096006; <http://dx.doi.org/10.1177/1352458508096006>.

Schmierer, K., Scaravilli, F., Altmann, D.R., Barker, G.J., Miller, D.H., 2004. Magnetization transfer ratio and myelin in postmortem multiple sclerosis brain. Ann. Neurol. 56 (3), 407–415. doi:10.1002/ana.20202; <http://dx.doi.org/10.1002/ana.20202>.

Schmierer, K., Tozer, D.J., Scaravilli, F., Altmann, D.R., Barker, G.J., Tofts, P.S., et al., 2007. Quantitative magnetization transfer imaging in postmortem multiple sclerosis brain. J. Magn. Reson. Imaging 26 (1), 41–51. doi:10.1002/jmri.20984; <http://dx.doi.org/10.1002/jmri.20984>.

Schmierer, K., Parkes, H.G., So, P.-W., An, S.F., Brandner, S., Ordidge, R.J., et al., 2010. High field (9.4 Tesla) magnetic resonance imaging of cortical grey matter lesions in multiple sclerosis. Brain 133 (Pt 3), 858–867. doi:10.1093/brain/awp335; <http://dx.doi.org/10.1093/brain/awp335>.

Schuh, C., Wimmer, I., Hametner, S., Haider, L., Van Dam, A.-M., Liblau, R.S., et al., 2014. Oxidative tissue injury in multiple sclerosis is only partly reflected in experimental disease models. Acta Neuropathol. 128 (2), 247–266. doi:10.1007/s00401-014-1263-5; <http://dx.doi.org/10.1007/s00401-014-1263-5>.

Serres, S., Anthony, D.C., Jiang, Y., Broom, K.A., Campbell, S.J., Tyler, D.J., et al., 2009. Systemic inflammatory response reactivates immune-mediated lesions in rat brain. J. Neurosci. 29 (15), 4820–4828. doi:10.1523/JNEUROSCI.0406-09.2009; <http://dx.doi.org/10.1523/JNEUROSCI.0406-09.2009>.

Serres, S., Anthony, D.C., Jiang, Y., Campbell, S.J., Broom, K.A., Khrapitchev, A., et al., 2009. Comparison of MRI signatures in pattern i and ii multiple sclerosis models. NMR Biomed. 22 (10), 1014–1024. doi:10.1002/nbm.1404; <http://dx.doi.org/10.1002/nbm.1404>.

Serres, S., Bristow, C., de Pablos, R.M., Merkler, D., Soto, M.S., Sibson, N.R., et al., 2013. Magnetic resonance imaging reveals therapeutic effects of interferon-beta on cytokine-induced reactivation of rat model of multiple sclerosis. J. Cereb. Blood Flow Metab. 33 (5), 744–753. doi:10.1038/jcbfm.2013.12; <http://dx.doi.org/10.1038/jcbfm.2013.12>.

Smith, S.A., Bulte, J.W.M., van Zijl, P.C.M., 2009. Direct saturation MRI: theory and application to imaging brain iron. Magn. Reson. Med. 62 (2), 384–393. doi:10.1002/mrm.21980; <http://dx.doi.org/10.1002/mrm.21980>.

Syha, R., Springer, F., Grözinger, G., Würslin, C., Ipach, I., Ketelsen, D., et al., 2014. Short-term exercise-induced changes in hydration state of healthy Achilles tendons can be visualized by effects of off-resonant radiofrequency saturation in a three-dimensional ultrashort echo time MRI sequence applied at 3 Tesla. J. Magn. Reson. Imaging 40 (6), 1400–1407. doi:10.1002/jmri.24488; <http://dx.doi.org/10.1002/jmri.24488>.

van Waesberghe, J.H., Kamphorst, W., De Groot, C.J., van Walderveen, M.A., Castelijns, J.A., Ravid, R., et al., 1999. Axonal loss in multiple sclerosis lesions: magnetic resonance imaging insights into substrates of disability. Ann. Neurol. 46 (5), 747–754. doi:10.1002/1531-8249(199911)46:5<747::aid-ana10>3.0.CO;2-4.

Vavasour, I.M., Li, D.K.B., Laule, C., Traboulsee, A.L., Moore, G.R.W., Mackay, A.L., 2007. Multi-parametric mr assessment of t(1) black holes in multiple sclerosis: evidence that myelin loss is not greater in hypointense versus isointense t(1) lesions. J. Neurol. 254 (12), 1653–1659. doi:10.1007/s00415-007-0604-x; <http://dx.doi.org/10.1007/s00415-007-0604-x>.

Vavasour, I.M., Laule, C., Li, D.K.B., Traboulsee, A.L., MacKay, A.L., 2011. Is the magnetization transfer ratio a marker for myelin in multiple sclerosis? J. Magn. Reson. Imaging 33 (3), 713–718. doi:10.1002/jmri.22441; <http://dx.doi.org/10.1002/jmri.22441>.

Zaaraoui, W., Deloire, M., Merle, M., Girard, C., Raffard, G., Biran, M., et al., 2008. Monitoring demyelination and remyelination by magnetization transfer imaging in the mouse brain at 9.4 t. MAGMA 21 (5), 357–362. doi:10.1007/s10334-008-0141-3; <http://dx.doi.org/10.1007/s10334-008-0141-3>.